Available online at www.sciencedirect.com

SciVerse ScienceDirect

Ceramics International 39 (2013) 1183–1188

CERAMICS INTERNATIONAL

www.elsevier.com/locate/ceramint

Influence of Ce^{3+} and Gd^{3+} co-doping on the structure and upconversion emission in hexagonal Ho^{3+} doped $NaYbF_4$ phosphors

Yongchang Li, Liwen Yang*, Yao Li, Suixi Yu, Ping Yang, Feng Jiang

Laboratory for Quantum Engineering and Micro-Nano Energy Technology and Faculty of Materials and Optoelectronic Physics, Xiangtan University, Hunan 411105, China

Received 30 May 2012; received in revised form 12 July 2012; accepted 12 July 2012
Available online 20 July 2012

Abstract

Hexagonal Ho^{3+} doped $NaYbF_4$ phosphors are synthesized via a hydrothermal method. The influence of Gd^{3+} and Ce^{3+} content on the phase structure and upconversion (UC) emission of $NaYbF_4$ phosphors is investigated by X-ray diffraction (XRD), transmission electron microscopy (TEM) and UC spectra. The results of XRD and TEM indicate that the solubility of Ce^{3+} in hexagonal $NaYbF_4$ is low due to the large difference of ionic radius between Ce^{3+} and Yb^{3+}. With help of Gd^{3+} co-doping (15 mol%), pure hexagonal $NaYbF_4$ phosphors with high doping concentration of Ce^{3+} (15 mol%) and small crystal size are obtained. When excited by a 980 nm laser diode, Ho^{3+} doped hexagonal $NaYb_{0.85}Gd_{0.15}F_4$ phosphors exhibit strong green UC emission at 540 nm and weak red one at 646 nm. UC luminescence tuning from green emission to red emission is observed in hexagonal Ho^{3+} doped $NaYb_{0.85}Gd_{0.15}F_4$ phosphors by co-doping with Ce^{3+} ions. The UC luminescence tuning phenomenon is attributed to two resonant energy transfer processes of $^5S_2/^5F_4(Ho^{3+})+{}^2F_{5/2}(Ce^{3+})\rightarrow{}^5F_5(Ho^{3+})+{}^5F_{7/2}(Ce^{3+})$ and $^5I_6(Ho^{3+})+{}^2F_{5/2}(Ce^{3+})\rightarrow{}^5I_7(Ho^{3+})+{}^5F_{7/2}(Ce^{3+})$ between Ho^{3+} and Ce^{3+}, which suppress the green emission at 540 nm, while promote the red one at 646 nm.

Keywords: Hydrothermal method; Upconversion; Upconversion luminescence tuning

1. Introduction

Lanthanide (Ln^{3+}) ions doped up-conversion (UC) materials attract more and more attention because of their potential applications in solid-state lasers [1], multi-color displays [2,3], optical processing sensors [4], solar cells [5], and especially, luminescencent labels for bioimaging and biomedicine [6–8]. At present, many host materials, such as oxides, phosphates, vanadates, fluorides, and chlorides, have an ability to demonstrate highly efficient multicolor UC emissions under the excitation of a near-infrared (NIR) laser diode with wavelength of 980 nm [9–12]. Among them, sodium lanthanide fluorides ($NaLnF_4$) have been considered as the most excellent hosts for various optically active Ln^{3+} ions since they possess a high refractive index and low phonon energy ($<400\ cm^{-1}$) leading to low nonradiative relaxation probability and consequently high luminescence efficiency of Ln^{3+} ions. For example, it has been demonstrated that multi-color UC emissions spanning infrared to deep ultraviolet including white light can be obtained from $NaYF_4$ and $NaGdF_4$ nanocrystals by precisely controlling the doping type and concentration of Ln^{3+} ion [8,10,13–16]. Very interestingly, in these systems, Ln^{3+} doping also has great effect on the crystal phase and size along with the UC emission. For instance, Liu and co-workers [3] demonstrated that the size reduction down to ten nanometers, phase transformation from cubic to hexagonal of $NaYF_4$ nanocrystals could be rationally tuned by introducing trivalent Gd^{3+} ions at precisely defined concentrations. Recently, Ln^{3+} doped $NaYbF_4$ nano- and micro-crystals were also found to exhibit intense multicolor UC emissions, such as ultraviolet, orange, yellow, green, cyan, blue, pink as well as near-infrared (NIR), under a

*Corresponding author.
E-mail address: ylwxtu@xtu.edu.cn (L. Yang).

0272-8842/$ - see front matter © 2012 Elsevier Ltd and Techna Group S.r.l. All rights reserved.
http://dx.doi.org/10.1016/j.ceramint.2012.07.042

single NIR (980 nm) laser irradiation benefited from the high Yb^{3+} content in the host [17]. On the other hand, Ce^{3+} ion is the most important activator in various fluoride and oxide materials because of its allowed $4f^n \rightarrow 4f^{n-1}5d$ optical transitions [18–20]. Although considerable interest has been focused upon the down-conversion luminescence of Ce^{3+}-doped luminescence materials under ultraviolet excitation, there have been only a few studies on the UC luminescence of Ce^{3+} ions and the effect of Ce^{3+} ions on the structure and UC emission of Ln^{3+} doped UC materials [21–23]. Previously, Chen et al. reported that co-doping of Ce^{3+} ions could lead to the color output from green to red in cubic $NaYF_4$ nanocrystals under the excitation of a 980 nm laser [21]. Wang et al. reported unusual UC emissions of Ho^{3+} ions in $Yb^{3+}/Ho^{3+}/Ce^{3+}$ co-doped $NaYF_4$ nanorods [22]. In this work, hexagonal Ho^{3+} doped $NaYbF_4$ phosphors are synthesized by a hydrothermal method using oleic acid as a stabilizing agent. The influence of Gd^{3+} and Ce^{3+} content on the phase structure and UC emission of $NaYbF_4$ phosphors is investigated in detail.

2. Experimental

The synthesis was carried out using commercially available reagents. The $Ln(NO_3)_3 \cdot 6\,H_2O$ with the grade of 99.99% were supplied by Sinopharm Chemical Reagent Company. All other chemicals were analytical grade and were used as received without further purification. In a typical synthesis, 2 ml of an aqueous solution containing 8.75 mmol NaOH, 12 ml alcohol and 15 ml oleic acid were added to a beaker sequentially under vigorous stirring to form a transparent homogeneous solution at room temperature. Then, 2.24 ml of 0.5 M $Ln(NO_3)_3$ (1.12 mmol) with pre-designed Yb^{3+}, Ho^{3+} and Ce^{3+} doping content were poured into the translucent solution under vigorous stirring and the obtained mixture was aged for 10 min at room temperature. At last, 5 ml of 1.2 M NaF (6 mmol) were added under vigorous stirring until a translucent solution was obtained. After agitating for another 30 min, the colloidal solution was transferred to a 50 ml stainless Teflon-lined autoclave. The reactions were conducted in an oven at 190 °C for 20 h. After the reaction, the products deposited on the bottom of the Teflon vessel were collected and washed with ethanol and deionized water several times to remove other remnants, and then dried at 70 °C for 24 h.

The crystal structures of the synthesized samples were determined by X-ray diffraction (XRD, D/Max 8550) using a copper K_α radiation source ($\lambda = 0.154$ nm) at 40 kV and 40 mA. The morphologies and microstructures were characterized by transmission electron microscopy (TEM, JEOL 2100) equipped with selected area electron diffraction (SAED) and an Oxford energy dispersive X-ray spectroscopy (EDS) system at an acceleration voltage of 200 kV. The TEM specimens were prepared by directly drying a drop of a dilute cyclohexane dispersion solution of the as-prepared products on the surface of a carbon-coated copper grid. The UC spectra were recorded on a spectrophotometer (R-500) under excitation by a 980 nm laser diode (LD) after the powder samples were compressed into smooth slices. The fluorescence spot of the parallel laser beam on the sample had a diameter of about 0.4 cm and the measurements were performed at room temperature. The UC photographic images of the samples were taken by a digital camera (Canon PowerShot A720, Japan) without adding any filter.

3. Results and discussion

The XRD patterns of $NaYbF_4$ samples with different concentrations of Ce^{3+} are shown in Fig. 1. Compare to the standard PDF card data, the XRD peaks from the sample without Ce^{3+} doing match well up to standard hexagonal $NaYbF_4$ (JCPDS 27-1427). From the XRD results, one can find that when the concentration of Ce^{3+} doping is less than 10 mol%, Ce^{3+} doping has no influence on the structure of hexagonal β-$NaYbF_4$ and no impurity phase can be detected. However, with increasing Ce^{3+} doping concentration beyond 15 mol%, a small amount of impurity phase, which originates from cubic $NaCeF_4$ (JCPDS 77-2043), appears. The results indicate that due to the large difference of ionic radius between Ce^{3+} ($r = 0.1283$ nm) and Yb^{3+} ($r = 0.1125$ nm) [24], the solubility of Ce^{3+} in hexagonal $NaYbF_4$ is rather low. Since the solubility of Ce^{3+} in $NaYbF_4$ strongly depends on the difference of its ionic radius, it can be imagined that co-doping of another Ln^{3+} ion, whose ionic radius is situated between Ce^{3+} and Yb^{3+} to bridging the gap of ionic radius, will increase the solubility of Ce^{3+} in $NaYbF_4$ host. Although several Ln^{3+} ions including Nd^{3+} ($r = 0.1249$ nm), Gd^{3+} ($r = 0.1193$ nm), Eu^{3+} ($r = 0.1206$ nm) and Sm^{3+} ($r = 0.1219$) [24] have an ability to bridging the gap of ionic radius between Ce^{3+} and Yb^{3+}, only Gd^{3+} favors UC emission due to its unique energy levels. In Gd^{3+} doped system, the lowest excited level ($^6P_{7/2}$) of Gd^{3+} is situated in ultraviolet region, which is far higher than most excited levels of

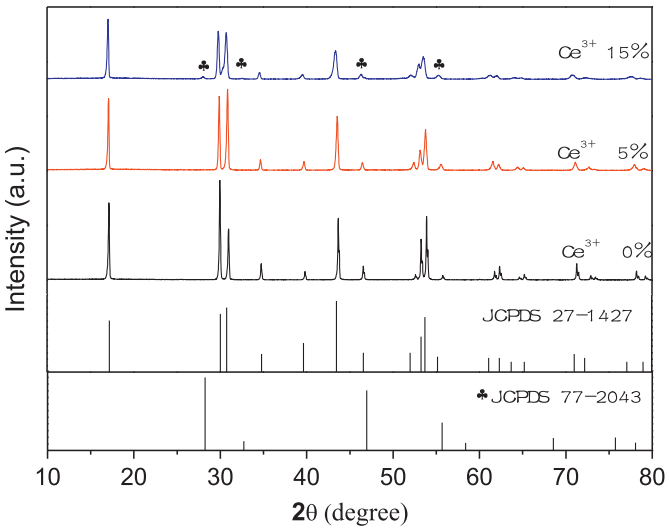

Fig. 1. XRD patterns of 0.25 mol% Ho^{3+} doped $NaYbF_4$ co-doping with different concentrations of Ce^{3+} ions.

Yb^{3+} and other luminescent Ln^{3+} ions of Er^{3+}, Ho^{3+} and Tm^{3+} involved in UC processes [3]. Thus, excitation energy loss through energy transfer (ET) from Yb^{3+}, Er^{3+}, Ho^{3+} and Tm^{3+} to 4f levels of Gd^{3+} can be avoided. Hence the presence of Gd^{3+} dopant ions at a broad concentration range has no obvious quenching effect on UC luminescence. In contrast, due to the quenching of excitation energy through efficient ET from Yb^{3+} and Er^{3+} to ^6F_J manifolds of Sm^{3+} or ^4I_J manifolds of Nd^{3+}, the intensity of visible UC luminescence is depressed notably in $NaYF_4$ host co-doping with Sm^{3+} or Nd^{3+} with doping concentration beyond 15 mol%. Fig. 2 shows the XRD results of Ce^{3+} (15 mol%) doped $NaYbF_4$ samples co-doping with different Gd^{3+} concentrations. One can see that when the Gd^{3+} doping concentration is beyond 15 mol%, all XRD peaks ascribed to cubic $NaCeF_4$ disappear and pure hexagonal $NaYbF_4$ forms. The results undoubtedly confirm our hypothesis.

The morphologies and microstructures of the samples are further examined by TEM observations. Fig. 3(a) shows typical low-magnified TEM image of Ho^{3+} (0.25 mol%) doped $NaYbF_4$ powder, displaying non-uniform morphology with diameter of about 1.5 μm. Fig. 3(b) shows typical low-magnified TEM image of Ho^{3+} doped $NaYbF_4$ powder co-doping with 15 mol% Ce^{3+}. Uniform rods with large size about 1.5 μm and small particles can be observed, implying the existence of two phases, which is consistent with the XRD results. Fig. 3(c) shows typical low-magnified TEM image of Ho^{3+} doped $NaYb_{0.85}Ce_{0.15}F_4$ sample co-doping with 15 mol% Gd^{3+}. Pure rods with size of 400 nm are observed, demonstrating the reduction of crystal size with Gd^{3+} doping. The phenomenon of size reduction is similar with that reported in $NaYF_4$ [3]. Further EDS results confirm that the main elemental components of Ho^{3+} doped $NaYb_{0.85}Gd_{0.15}F_4$ sample co-doping with 15 mol% Ce^{3+} [see Fig. 3(d)] are Na, Yb, Ce, Gd and F. The mol ratio of Ce is about

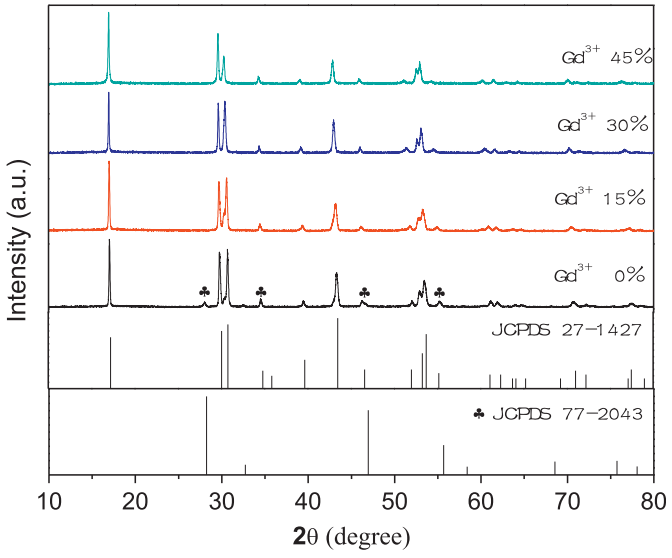

Fig. 2. XRD results of 0.25 mol% Ho^{3+} doped $NaYb_{0.85}Ce_{0.15}F_4$ co-doping with different Gd^{3+} concentrations.

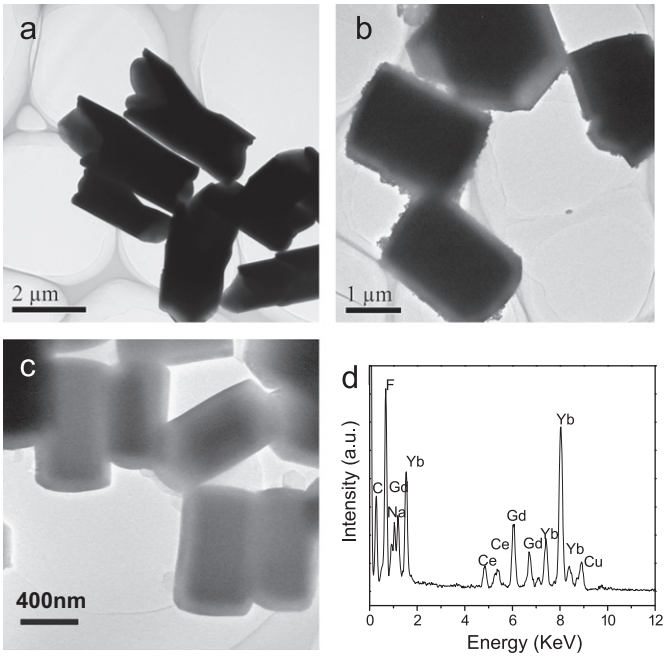

Fig. 3. (a)–(c) Typical TEM images of 0.25 mol% Ho^{3+} doped $NaYbF_4$, $NaYb_{0.85}Ce_{0.15}F_4$, and $NaYb_{0.7}Ce_{0.15}Gd_{0.15}F_4$, respectively. (d) EDS spectrum of 0.25 mol% Ho^{3+} doped $NaYb_{0.7}Ce_{0.15}Gd_{0.15}F_4$.

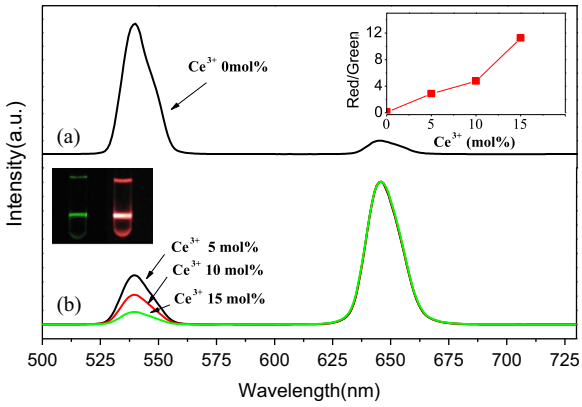

Fig. 4. Normalized UC spectra of 0.25 mol% Ho^{3+} doped $NaYb_{0.85}Gd_{0.15}F_4$ codoping with different Ce^{3+} concentrations under the excitation by a 980 nm LD. The inset shows the intensity ratio of red to green UC emission as a function of Ce^{3+} ions. (For interpretation of the references to color in this figure legend, the reader is reffered to the web version of this article.)

14.3%, which is very close to the nominal Ce^{3+} concentration, implying that all Ce^{3+} ions are doped in $NaYbF_4$ host and the solubility of Ce^{3+} in $NaYbF_4$ host increases with Gd^{3+} co-doping.

Fig. 4 presents the normalized UC spectra of Ho^{3+} (0.25 mol%) doped $NaYb_{0.85}Gd_{0.15}F_4$ co-doping different Ce^{3+} concentrations under the excitation of a 980 nm laser. All spectra have been normalized according to the peak intensity of red emission at 650 nm. From the spectra of the sample without Ce^{3+} [see Fig. 4(a)], two strong emission bands can be observed. One is green emission centered on 540 nm and the other is red one centered on

646 nm, which correspond to the $^5F_5 \rightarrow {}^5I_8$ and $^5S_2/^5F_4 \rightarrow {}^5I_8$ transitions of Ho^{3+}, respectively. Especially, the intensity of green emission is stronger than that of red one and the ratio of the former to the latter is about 9.6. Fig. 4(b) presents the normalized UC spectra of Ho^{3+} (0.25 mol%) doped $NaYb_{0.85}Gd_{0.15}F_4$ with different Ce^{3+} concentrations. One can see that after the addition of Ce^{3+}, the spectra change notably and the red emission at 646 nm becomes stronger compared with the green one at 540 nm. With increasing Ce^{3+} concentrations, the ratios of the intensity of red emission to that of green one become larger and larger [see the inset of Fig. 4(a)]. When the Ce^{3+} concentration is about 15 mol%, almost single red emission is obtained. The inset of Fig. 4(b) shows the digital images of $NaYb_{0.85}Gd_{0.15}F_4$ phosphors doped with 0.25 mol% Ho^{3+} and further tri-doped with 15 mol% Ce^{3+} ions in cyclohexane under 980 nm laser excitation. Pure green and red UC emissions are clearly observed, which agree well with the spectral data. The results imply that luminescence tuning from green emission to red emission can be realized in Ho^{3+} doped $NaYb_{0.85}Gd_{0.15}F_4$ phosphors via Ce^{3+} codoping. Fig. 5 shows the normalized UC spectra of Ho^{3+} (1 mol%) doped $NaYbF_4$ samples co-doping with different Gd^{3+} concentrations. From the spectra and the ratios of the intensity of red emission to that of green one (see the inset of Fig. 5), no obvious luminescence tuning from green emission to red emission is observed. The results exclude the possibility of luminescence tuning originates from the role of Gd^{3+} ions, and confirm that it must be associated with the interaction between Ho^{3+} and Ce^{3+}.

To further clarify the UC mechanisms, the power dependent UC behaviors of the observed emissions are systematically investigated. Generally, for unsaturated UC processes, the UC luminescence intensity (I_{UC}) is related to the pump infrared one (I_{IR}) via the formula, $I_{UP} \propto I_{IR}^n$, where n is the pump photon number required to populate the upper emitting level and its value can be obtained from the slope of the line in the plot of $\log(I_{UP})$ versus $\log(I_{IR})$[15]. Fig. 6(a) presents the double logarithmic plots of the emission intensity as a function of excitation power for the $^5F_5 \rightarrow {}^5I_8$ and $^5S_2/^5F_4 \rightarrow {}^5I_8$ emissions in 0.25 mol% Ho^{3+} doped $NaYb_{0.85}Gd_{0.15}F_4$ sample. The slope values of the linear fits with the experimental data are 1.52 and 1.71 for the observed green emission and red emissions, respectively. Similarly the slope values for green emission and red emissions in 0.25 mol% Ho^{3+} and 15 mol% Ce^{3+} co-doped $NaYb_{0.85}Gd_{0.15}F_4$ sample are 1.42 and 1.78 for the observed green emission and red emissions [see Fig. 6(b)], respectively. The results indicate that two pump photons are necessary to produce the green and red emissions in $NaYbF_4$ samples and the Ce^{3+} co-doping has no obvious effect on the required photon number of UC process.

Fig. 7 shows energy levels of Yb^{3+}, Ho^{3+} and Ce^{3+} ions as well as the proposed UC mechanisms. For the green emission in Ho^{3+} doped $NaYb_{0.85}Gd_{0.15}F_4$ sample, firstly the Ho^{3+} is excited from the ground state to the $^5I_6$ state through ET process from excited Yb^{3+} ions. Subsequently, the $^5I_6$ state is further excited to $^5S_2/^5F_4$ state through another ET process from excited Yb^{3+} ions. When the $^5S_2/^5F_4$ state is radiatively decayed to the ground state, the green luminescence is generated. For the red emission from the $^5F_5$ state, there are two channels to populate it. One is that the $^5I_7$ state of the Ho^{3+} populated via a multiphonon nonradiative relaxation from the $^5I_6$ state is further excited to the $^5F_5$ state through one ET process from excited Yb^{3+} ions. The other is that the $^5S_2/^5F_4$ state relaxes to $^5F_5$ state via a multiphonon nonradiative relaxation. It should be noted that these two nonradiative relaxations should occur inefficiently, since both energy gaps are about 3000 cm^{-1}, which is much higher than the maximum phonon energy of $NaYbF_4$. As a result, the red emission is relatively weak,

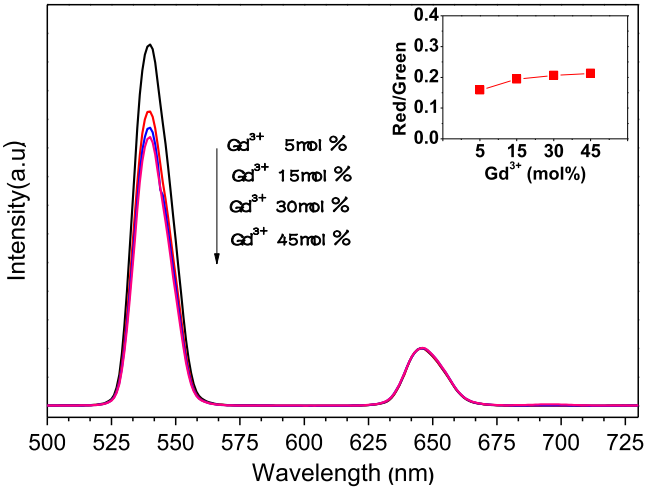

Fig. 5. Normalized UC spectra of the $NaYbF_4$ doped with 1 mol% Ho^{3+} and different Gd^{3+} concentrations under the excitation of a 980 nm LD. The inset shows the intensity ratio of red to green UC emission as a function of Gd^{3+} ions. (For interpretation of the references to color in this figure legend, the reader is reffered to the web version of this article.)

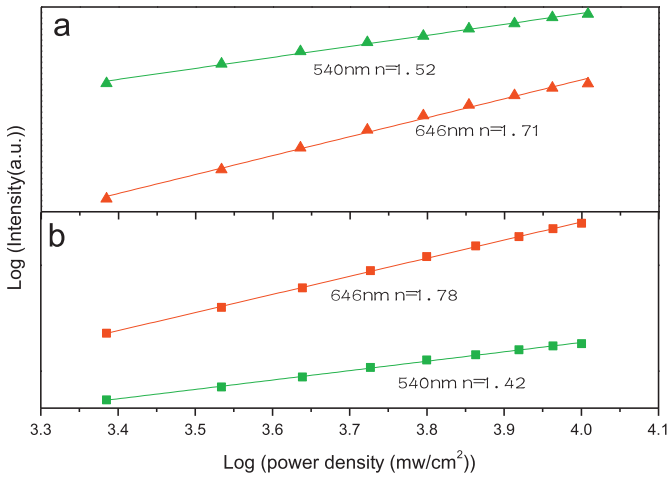

Fig. 6. Double logarithmic plots of the emission intensity as a function of excitation power for the $^5F_5 \rightarrow {}^5I_8$ and $^5S_2/^5F_4 \rightarrow {}^5I_8$ emissions in 0.25 mol% Ho^{3+} doped $NaYb_{0.85}Gd_{0.15}F_4$ (a) and $NaYb_{0.7}Gd_{0.15}Ce_{0.15}F_4$ (b).

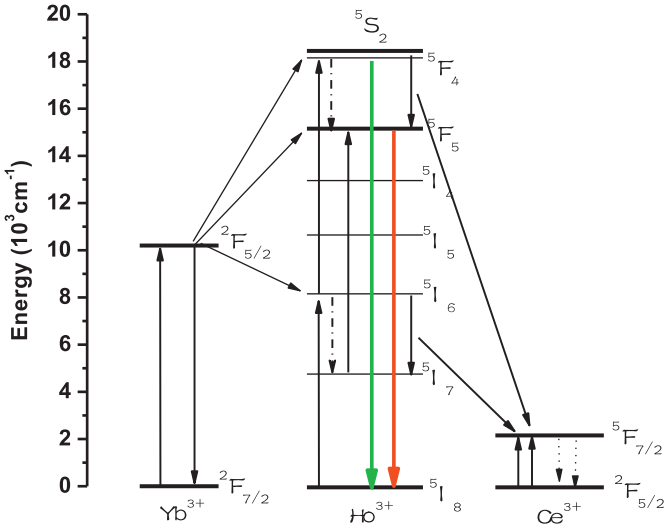

Fig. 7. Energy level diagrams of Yb^{3+}, Ho^{3+} and Ce^{3+} as well as proposed UC mechanisms under the excitation of a 980 nm LD.

which is consistent with the experimental observation. As for the UC mechanisms in Ho^{3+} doped $NaYb_{0.85}Gd_{0.15}F_4$ sample co-doping Ce^{3+}, the green emission is produced via the aforementioned UC processes since Ce^{3+} ion has an exclusive small energy gap of about 3000 cm^{-1} between its excited $^5F_{7/2}$ state and the ground $^2F_{5/2}$ state, which only affects ET processes that involve similar energy gaps according to the energy conservation law. However, the energy gaps between $^5F_{7/2}$ and $^2F_{5/2}$ state of Ce^{3+} is very close to those attributed to the population of the $^5F_5$ state via multiphonon nonradiative relaxation. Hence, resonant ET processes of $^5S_2/^5F_4(Ho^{3+})+^2F_{5/2}(Ce^{3+})\rightarrow{}^5F_5(Ho^{3+})+^5F_{7/2}(Ce^{3+})$ and $^5I_6(Ho^{3+})+^2F_{5/2}(Ce^{3+})\rightarrow{}^5I_7(Ho^{3+})+^5F_{7/2}(Ce^{3+})$ occur easily. These two resonant ET processes can transfer populations from the green-emitting $^5S_2/^5F_4$ state and its intermediate $^5I_6$ state to the red-emitting $^5F_5$ state and its intermediate $^5I_7$ state, respectively [21]. Those changes not only weaken the green emission, but also promote the red one, thereby leading to luminescence tuning from green emission to red one via Ce^{3+} co-doping.

4. Conclusions

Hexagonal Ho^{3+} doped $NaYbF_4$ phosphors are synthesized by a hydrothermal method. The XRD and TEM results indicate that the solubility of Ce^{3+} in hexagonal $NaYbF_4$ is low due to the large difference of ionic radius between Ce^{3+} and Yb^{3+}. With help of Gd^{3+} co-doping (15 mol%), pure hexagonal $NaYbF_4$ phosphors with high doping concentration of Ce^{3+} (15 mol%) and small crystal size are obtained. Under the excitation of a 980 nm laser, strong green UC emission at 540 nm and weak red one at 646 nm is observed in hexagonal Ho^{3+} doped $NaYb_{0.85}Gd_{0.15}F_4$ phosphors. Luminescence tuning from green emission to red one is obtained in pure hexagonal Ho^{3+} doped $NaYb_{0.85}Gd_{0.15}F_4$ phosphors by co-doping with Ce^{3+} ions. The UC luminescence tuning phenomenon is atributed to two resonant ET processes of $^5S_2/^5F_4(Ho^{3+})+^2F_{5/2}(Ce^{3+})\rightarrow{}^5F_5(Ho^{3+})+^5F_{7/2}(Ce^{3+})$ and $^5I_6(Ho^{3+})+^2F_{5/2}(Ce^{3+})\rightarrow{}^5I_7(Ho^{3+})+^5F_{7/2}(Ce^{3+})$ between Ho^{3+} and Ce^{3+}, which suppress the green emission at 540 nm, while promote the red one at 646 nm. Our results indicate that hexagonal Ln^{3+} doped $NaYbF_4$ phosphors have potential applications in color displays and multicolor fluorescent labels.

Acknowledgements

This work was supported by the Grants from National Natural Science Foundation of China (No 51172191) and the Open Fund based on the innovation platform of Hunan colleges and universities (No. 11K060).

References

[1] F. Auzel, Upconversion and anti-stokes processes with f and d ions in solids, Chemical Reviews 104 (2004) 139–174.
[2] J. Hao, J. Gao, Abnormal reduction of Eu ions and luminescence in CaBO: Eu thin films, Applied Physics Letters 85 (2004) 3720–3722.
[3] F. Wang, Y. Han, C. Lim, Y. Lu, J. Wang, J. Xu, H. Chen, C. Zhang, M. Hong, X. Liu, Simultaneous phase and size control of upconversion nanocrystals through lanthanide doping, Nature 463 (2010) 1061–1065.
[4] C. Jacinto, M. Vermelho, E. Gouveia, M. de Araujo, P. Udo, N. Astrath, M. Baesso, Pump-power-controlled luminescence switching in Yb^{3+}/Tm^{3+} co-doped water-free low silica calcium aluminosilicate glasses, Applied Physics Letters 91 (2007) 071102.
[5] B. van der Ende, L. Aartsa, A. Meijerink, Lanthanide ions as spectral converters for solar cells, Physical Chemistry Chemical Physics 11 (2009) 11081–11095.
[6] F. Wang, X. Liu, Recent advances in the chemistry of lanthanide-doped upconversion nano-crystals, Chemical Society Reviews 38 (2009) 976–989.
[7] F. Wang, D. Banerjee, Y. Liu, X. Chen, X. Liu, Upconversion nanoparticles in biological labeling, imaging, and therapy, Analyst 135 (2010) 1839–1854.
[8] J. Zhou, Z. Liu, F. Li, Upconversion nanophosphors for small-animal imaging, Chemical Society Reviews 41 (2012) 1323–1349.
[9] C. Li, J. Lin, Rare earth fluoride nano-/micro-crystals: synthesis, surface modification and application, Journal of Materials Chemistry 20 (2010) 6831–6847.
[10] M. Haase, H. Schäfer, Upconverting nanoparticles, Angewandte Chemie International Edition 50 (2011) 5808–5829.
[11] V. Mahalingam, F. Vetrone, R. Naccache, A. Speghini, J. Capobianco, Colloidal Tm^{3+}/Yb^{3+}-doped $LiYF_4$ nanocrystals: multiple luminescence spanning the UV to NIR regions via low energy excitation, Advances in Materials 21 (2009) 4025–4028.
[12] V. Mahalingam, F. Vetrone, R. Naccache, A. Speghini, J. Capobianco, Structural and optical investigation of colloidal Ln^{3+}/Yb^{3+} co-doped KY_3 F_{10} nanocrystals, Journal of Materials Chemistry 19 (2009) 3149–3152.
[13] F. Wang, X. Liu, Upconversion multicolor fine-tuning: visible to near-infrared emission from lanthanide-doped $NaYF_4$ nanoparticles, Journal of the American Chemical Society 130 (2008) 5642–5643.
[14] L. Yang, Y. Zhang, J. Li, Y. Li, J. Zhong, P.K. Chu, Magnetic and upconverted luminescent properties of multifunctional lanthanide doped cubic $KGdF_4$ nanocrystals, Nanoscale 2 (2010) 2805–2810.
[15] L.W. Yang, H.L. Han, Y.Y. Zhang, J.X. Zhong, White emission by Frequency up-conversion in Yb^{3+}–Ho^{3+}–Tm^{3+} triply doped hexagonal $NaYF_{4n}$ nanorods, Journal of Physical Chemistry C 113 (2009) 18995–18999.

[16] L.W. Yang, Y. Li, Y.C. Li, J.J. Li, J.H. Hao, J.X. Zhong, P.K. Chu, Quasi-seeded growth, phase transformation, and size tuning of multifunctional hexagonal $NaLnF_4$ (Ln=Y, Gd, Yb) nanocrystals via in situ cation-exchange reaction, Journal of Materials Chemistry 22 (2012) 2254–2262.

[17] D. Chen, Y. Yu, F. Huang, A. Yang, Y. Wang, Lanthanide activator doped $NaYb_{1-x}Gd_xF_4$ nanocrystals with tunable down-, up-conversion luminescence and paramagnetic properties, Journal of Materials Chemistry 21 (2011) 6186–6192.

[18] G. Buhler, C. Feldmann, Microwave assisted synthesis of luminescent $LaPO_4$: Ce, Tb nanocrystals in ionic liquids, Angewandte Chemie International Edition 45 (2006) 4864–4867.

[19] G. Xu, Z. Zheng, W. Tang, Y. Wu, Luminescence property of Ce^{3+}-doped silica decorated with S_2- and C_l-anions, Journal of Luminescence 126 (2007) 475–480.

[20] R. Reisfeld, A. Patra, G. Panczer, M. Gaft, Spectroscopic properties of cerium in sol–gel glasses, Optical Materials 13 (1999) 81–88.

[21] G. Chen, H. Liu, G. Somesfalean, H. Liang, Z. Zhang, Upconversion emission tuning from green to red in Yb_{3+}/Ho_{3+}-codoped $NaYF_4$ nanocrystals by tridoping with Ce_{3+} ions, Nanotechnology 20 (2009) 385704.

[22] G. Wang, Q. Peng, Y. Li, Luminescence tuning of upconversion nanocrystals, Chemistry A European Journal 16 (2010) 4923–4931.

[23] K. Zhang, C. Zhao, H. Zhong, Y. Hang, Influence of Ce_{3+} on the luminescence properties of Er_{3+}/Yb_{3+}: YVO_4 crystals, Optical Materials 33 (2011) 788–790.

[24] R.D. Shannon, Revised effective ionic radii and systematic studies of interatomic distances in halides and chalcogenides, Acta Crystallogr. A 32 (1976) 751–767.